CHANNEL ESTIMATION BASED ADAPTIVE EQUALIZATION/DIVERSTIY COMBINING FOR TIME-VARYING DISPERSIVE CHANNELS

Heung-No Lee and Gregory J. Pottie

The authors are with the Department of Electrical Engineering,

University of California, Los Angeles

Abstract - We propose a novel reduced dimension channel impulse response (CIR) estimation procedure. Since the overall CIR is a convolution of the transmit and the channel filter, the number of unknown parameters can be reduced also reducing the training sequences. For symbol detection in fast fading, we introduce a new DFE coefficients computation algorithm which incorporates the channel variation during the decision delay into the minimum mean square error criterion, which we refer as to the non-Toeplitz DFE (NT-DFE). Finally, we show the feasibility of a suboptimal receiver which has complexity less than that of recursive least squares type adaptations with performance close to the optimal NT-DFE.

I. INTRODUCTION

The receiver design for frequency selective fading channels is quite demanding in fast fading. For example, in IS-54, assuming a mobile moves at a maximum highway speed of 120 *km/hr*, the maximum normalized Doppler fading rate $f_{dm}T$ (the product of the maximum Doppler fading rate and the symbol period) reaches up to 0.0042 [1]. This implies that the minimum time between the two fading nulls is 5 *ms* ($1/2f_{dm}$) which is even shorter than the proposed burst length of 6.7 *ms*.

For the estimation and tracking of such fast changing channels, the block adaptive strategy was reported more effective than the conventional symbol by symbol adaptation such as least mean squares (LMS) or even recursive least squares (RLS) [2,3,4,5,6]. The snap-shot channel estimates are computed exclusively from training symbols. Then, the channel tracking during the data segments is performed by interpolating a set of the snap-shot channel impulse response (CIR) estimates. With the interpolated CIR estimates, the receiver filter coefficients are computed.

In this paper, we extend previous results on periodic channel estimation based on the diversity combining decision feedback equalizer. In section II, we describe the system. Section III discusses a new reduced channel estimation method which exploits the fact that the overall channel is a convolution of the shaping and the time-varying channel filter. We also explain the interpolation procedures. In IV, we describe a new DFE coefficient computation algorithm to deal with very fast fades. In V, we show through computer simulations the performance of the receiver. Finally, the feasibility of a low computational complexity but suboptimal solution is discussed.

II. SYSTEM DESCRIPTION

A complex baseband representation of the system is shown in Fig. 1. The transmit filter f is a square root raised cosine (SRRC) filter with a roll-off $\beta = 0.35$. L independent diversity received signals corrupted by additive complex-valued white Gaussian noise (AWGN) are assumed to be available. Since the received signal $x_l(t)$ at each diversity branch is bandlimited with an excess bandwidth of $(1+\beta)(1/T)$, *T/2-spaced* sampling is considered, i.e., $x_l(k) := x_l(t = kT/2)$. Then, the impulse responses of the transmit and the channel filters could be realized with *T/2-spaced* tapped delay line FIR filters [5]. Then, $I(k)$ denotes the zero stuffed QPSK/DQPSK symbol sequence, where k will denote the *T/2*-spaced epoch index. During the periodic training mode, $I(k)$ represents the training symbols. Each filter coefficient is stored in the corresponding column vectors. Hence, each time-varying channel impulse response $b_l(\tau;t)$ is expressed as an $[N_R \times 1]$ column vector having time-varying coefficients $\underline{b}_l(k) = [b_{b0}(k) \ldots b_{bN_R-1}(k)]^T$, where N_R is the number of the time-varying channel taps ($N_R = 3$ in this paper). The noise $n_l(t)$ is also assumed to be *T/2-spaced* sampled and the sampled noise sequence $n_l(k)$ has a variance σ_n^2.

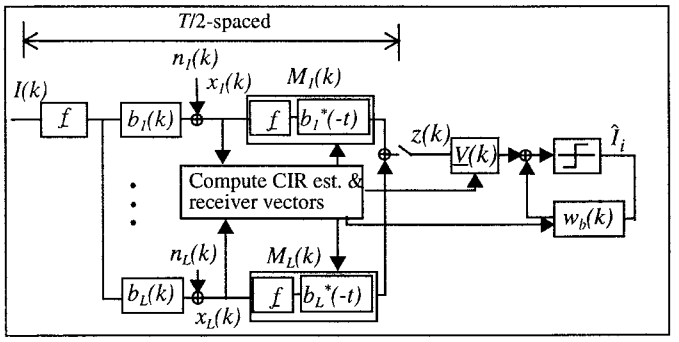

Fig. 1 Block diagram of the complete system

The mountainous terrain multipath delay profile (MT-MPDP) in [5] exhibits the worst delay spreads among the various land mobile MPDPs [6]. Thus, we use the same MT-MPDP, three fixed spaced (*T/2-spaced*) relative rms powers of 0dB, -5dB, -15dB and with a normalized rms delay spread of about 1/4. We assume that the channel taps undergo Rayleigh amplitude fading according to Jake's model [8] and are mutually uncorrelated [7]. In this paper, assuming a symbol rate ($1/T$) of 24 *ksps* the fast fading corresponds to $fdm = 100$ *Hz* ($fdmT = 0.0042$) and slow fading to $fdm = 10$ *Hz* ($fdmT = 0.00042$).

III. SNAP-SHOT CHANNEL ESTIMATION

At the end of each periodic training segment, a snap-shot channel estimation is performed. That is, during the observation interval, mT, we assume the channel is effectively fixed. Consequently, we drop the time index of the channel vector. Similarly, for the overall channel, $g(k) = \underline{f} * \underline{b}(k) = \underline{f} * \underline{b} = \underline{g}$ during the observation $k = 0, 1, \ldots, 2m-1$.

A. Estimation Equations

The use of bandwidth efficient shaping filters increases the effective span of the channel impulse response. Thus we shall estimate the overall channel impulse response (CIR). We truncate the length of the CIR to Nc symbol periods, i.e. $2Nc$ *T/2-spaced* taps, in the estimation model in order to reduce the length of the training sequence. The resultant modelling errors will be attributed to the overall channel estimation

errors. Then, for our double sampling system the received signal during training is described as,

$$x(k) \cong \sum_{i=0}^{2Nc-1} g_i I(k-i) + n(k) , \quad (1)$$

where $I(k)$ is a zero stuffed training sequence, i.e, QPSK/DQPSK symbols for even k and 0 for odd k. Using (1) the number of unknowns are the $2Nc$ coefficients of $\underline{g}$. However, using the fact that the overall filter is a cascade of the transmit and the channel filters, (1) can be rewritten as

$$x(k) \cong \sum_{i=0}^{2Nc-1} \sum_{j=0}^{N_R-1} f_{ij} b_j I(k-i) + n(k) , \quad (2)$$

where the matrix elements $[f_{ij}]$ are completely determined for a SRRC filter with a roll-off β. Then, the number of unknowns can be reduced to N_R. Having obtained the estimates of $\underline{b}$, estimates of overall channel can be obtained.

It can be shown that the received signals during the observation can be partitioned into even and odd indexed sequences and that each sequence yields a *T-spaced* channel estimation problem that can be described as

$$\underline{r} = XF\underline{b} + \underline{n} , \quad (3)$$

where $\underline{r}$ is a observation vector for even or odd sequences. X is a $[m \times Nc]$ Toeplitz matrix whose elements are just delayed versions of the training symbols such that

$$X = \begin{bmatrix} I(0) & I(-2) & \dots & I(-2(Nc-1)) \\ I(2) & I(0) & \dots & I(-2(Nc-2)) \\ \dots & \dots & \dots & \dots \\ I(2(m-1)) & I(2(m-2)) & \dots & I(2(Nc+m-2)) \end{bmatrix}.$$

Thus, the length of training sequence Nt is $Nc + m - 1$. The $[Nc \times N_R]$ SRRC matrix F can be readily determined for even or odd sequences once the roll-off β is determined. The $[m \times 1]$ noise vector $\underline{n}$ is a multivariate Gaussian vector with a zero mean vector and a covariance matrix of $R_n = \sigma_n^2 \mathbf{I}$, where $\mathbf{I}$ denotes for an identity matrix of appropriate dimension. From the even and the odd part, two estimates of $\underline{b}$ can be obtained. We choose the one that yields a smaller theoretical mean square estimation error for a given training sequence.

B. Three Classical Estimates of $\underline{b}$ and their Mean Square Errors

Given the estimation model (3), least squares estimation (LSE), maximum likelihood estimation (MLE), and maximum *a posteriori* estimation (MAP) criteria are considered for the estimation of $\underline{b}$. In the derivations of estimators, the training sequence matrix X is assumed to be fixed both in the contents and in the dimension and only cases for $m \geq N_R$ will be considered in this paper. Moreover, the inverse matrices in each estimation operator to be derived are assumed to be well defined. We use the optimal training sequences discussed in [2] and find the inverses of the operators are well defined.

First, if there is no *a priori* statistical knowledge about the noise and the channel, the LSE of $\underline{b}$ might be considered, i.e.,

$$\hat{\underline{b}}_{LSE} := \arg\min_{\underline{b}} |r - XF\underline{b}|^2 , \quad (4)$$
$$= (F^H X^H XF)^{-1} (XF)^H \underline{r}$$

where the superscript 'H' implies the conjugate transpose operation of a matrix and "arg" denotes the argument. This results in the lowest complexity estimator among the three. The $[N_R \times m]$ matrix $(F^H X^H XF)^{-1} (XF)^H$ can be precomputed and stored and the estimates will be obtained by multiplying it with the observation vector $\underline{r}$.

The MLE of $\underline{b}$ can be obtained as follows,

$$\hat{\underline{b}}_{ML} := \arg\max_{\underline{b}} (p(\underline{r}|\underline{b})) \quad (5)$$
$$= \arg\max_{\underline{b}} \left[-(\underline{r} - XF\underline{b}) R_n^{-1} (\underline{r} - XF\underline{b})^H \right]$$

setting the gradient of the quadratic term equal to zero, we obtain

$$\hat{\underline{b}}_{ML} = \left(F^H X^H R_n^{-1} XF \right)^{-1} \left(X^H F^H R_n^{-1} \right) \cdot \underline{r} . \quad (6)$$

Thus, the MLE requires the second order statistics of the noise, such as the noise covariance matrix R_n. The error covariance matrix (also a mean square error matrix for MLE and LSE since they are unbiased) is

$$\Theta_{ML} := E(\hat{\underline{b}}_{ML} - E(\hat{\underline{b}}_{ML}))(\hat{\underline{b}}_{ML} - E(\hat{\underline{b}}_{ML}))^H \quad (7)$$
$$= \left(F^H X^H R_n^{-1} XF \right)^{-1} .$$

It can be shown that this error covariance matrix of (7) meets the Cramer-Rao lower bound (unbiased class). Thus, $\hat{\underline{b}}_{ML}$ is the best linear unbiased estimator for the estimation problem of (5). MLE is good when the noise is correlated and the autocorrelation function of the noise is known. Also note that interpreting the R_n^{-1} as the optimal weighting matrix, the MLE criterion of (5) can be interpreted as the optimally weighted LS estimation of $\underline{b}$. Thus, the MLE also minimizes the square residual errors, $\underline{r} - XF\underline{b}$, but not the estimation errors, $\hat{\underline{b}}_{ML} - \underline{b}$. In our problem, however, $R_n = \sigma_n^2 \mathbf{I}$ is assumed, thus LSE and MLE produce identical results, i.e.,

$$\Theta_{ML} = \sigma_n^2 (F^H X^H XF)^{-1} = \Theta_{LSE} \quad \text{and} \quad \hat{\underline{b}}_{ML} = \hat{\underline{b}}_{LSE} . \quad (8)$$

An estimator which directly minimizes the mean square estimation errors of $\underline{b}$ requires *a priori* statistical knowledge of $\underline{b}$ (Bayes estimates). In our case, the noise vector is a multivariate Gaussian, and thus the posterior density $p(\underline{b}|\underline{r})$ is also a Gaussian in which case the mode and the mean coincide. Then, the MAP estimator of $\underline{b}$ amounts to the minimum mean square estimator of $\underline{b}$. The MAP estimate is obtained from

$$\hat{\underline{b}}_{MAP} := \arg\max_{\underline{b}} (p(\underline{b}|\underline{r})) = \arg\max_{\underline{b}} \left(\frac{p(\underline{b}, \underline{r})}{p(\underline{r})} \right) . \quad (9)$$

With some algebraic manipulations of the posterior density, we obtain the MAP estimator as

$$\hat{\underline{b}}_{MAP} = E\{\underline{b}|\underline{r}\} \quad (10)$$
$$= R_b (F^H X^H) (XFR_b F^H X^H + R_n)^{-1} \underline{r}$$

where $R_b = E\{\underline{b}\underline{b}^H\}$.

Since the MAP estimator is a biased estimator, we directly obtain the mean square error matrix as

$$\Theta_{MAP} = \left(R_b - B^+ XFR_b \right) , \quad (11)$$

where $B^+ := R_b (F^H X^H) (XFR_b F^H X^H + R_n)^{-1}$.

Note that MAP not only requires R_n but also R_b. Diagonal elements of the channel correlation matrix R_b are the average powers of the corresponding paths, the MT-MPDP defined in section II, which we assumed estimated. Moreover, all off-diagonal elements are assumed to be zero valued from the wide-sense stationary uncorrelated scattering of the multi-path components.

In Fig. 2, the performance of the channel estimators, MLE and MAP, in terms of the mean square channel estimation errors (MSCEE) are assessed both in theory and in simulation for $(Nt, Nc) = (11, 6)$. Theoretical MSCEE are obtained from $trace\{\Theta\}$ of (8) or (11). We notice that the MLE asymtotically reaches the performance of MAP. For the simulation MSCEE calculations, the channel estimates at the end of the training observation window are compared with the true $\underline{b}(k)$, where k is the center epoch in the window. In slow fading, for $(Nt, Nc) = (11, 6)$ the simulation curves are very close to the theory. This suggests that the truncation at $Nc = 6$ is sufficient. On the other hand, fast fading curves start to deviate from the slow fading curves at 30dB for both ML and MAP. These deviations are due to the snap-shot channel estimation

assumption that during the observation periods the channel is fixed.

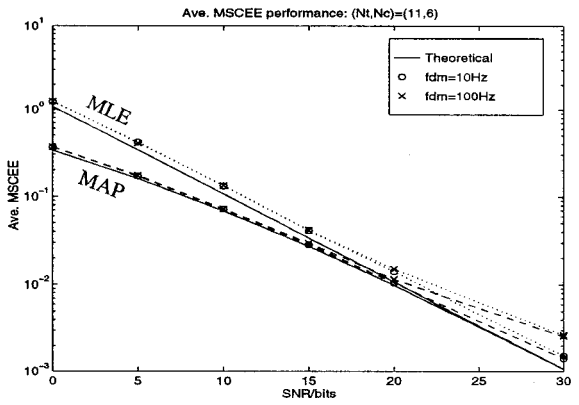

Fig. 2 Mean square channel estimate errors.

C. Channel Tracking by Interpolation

Channel tracking by interpolation provides the channel state information during the decision delay which would not be the case for a recursive type tracking which relies upon the detected symbol to update the channel state. Thus, receiver coefficients can be computed more robustly. Obviously, the cost is the interpolation delay.

In order to perform interpolations, first the frequency of channel estimation or the length of a frame B needs to be determined, where a frame consists of a training block (Nt) and a data block. According to the sampling theorem, B should satisfy $B \le 1/(2f_{dm}T)$. For instance, if $f_{dm}T = 0.0042$, the shortest null to null distance of a fading tap is about 240 symbols. Thus, B should be less than 120 symbols. Q (even integer) estimates are used for interpolation - Q/2 estimates of the past channel and Q/2 of the future. Thus, the interpolation delay should be at least (Q/2)B symbols. For detection of the data segment at the center of the Q consecutive frames, an interpolation over the Q consecutive estimated channel vectors is performed to obtain a channel vector at every *T/2-spaced* epoch. We use a sinc function ($\sin x/x$) for interpolation [5]. We use $B = 80$ and $Q = 4$ in this paper.

IV. OPTIMUM DIVERSITY COMBINING DFE

In this section, we discuss how to compute receiver coefficients using the estimates of the channel impulse response. We reformulate the Wiener-Hopf equations incorporating the channel variation during the decision delay into the minimum mean square detection error criterion [9]. The following summarizes the result of the derivation.

L diversity output signals can be combined using a matched filter at each branch and then the combined signal can be fed to the front-end of a feedforward filter (Fig. 1). The matched filtering at each branch is possible since we estimate the channel. Then, the L *T/2-spaced* diversity combining DFE can be treated as a single channel *T-spaced* DFE problem. That is, *T-spaced* sampled $z(n)$ can be described as,

$$z(n) = \underline{\psi}(n)^T \underline{I}(n) + \nu(n) , \qquad (12)$$

where the *T-spaced* summed channel autocorrelation function (SCAF) vector $\underline{\psi}(n)$ connotes the equivalent channel; $\nu(n)$ is the *T*-spaced equivalent noise which has $\sigma_n^2 \cdot \underline{\psi}(n)$ as its autocorrelation function; $I(k)$ now represents symbols without zero stuffing.

The decision delay Δ is defined as,

$$\Delta = N_g + 2(N_f - 1) , \qquad (13)$$

where N_g (even) is the number of *T/2-spaced* matched filter taps and N_f is the number of the *T-spaced* feedforward taps in $\underline{V}$. The matched filtered NT-DFE solution [9] on (12) can now be summarized as follows. For the following, assume $n = 0$ as the current epoch.

The $[N_g \times 1]$ matched filter vector can be implemented as,

$$\underline{M}_l = \left[g^*_{l,N_g-1}(-1) \;\; g^*_{l,N_g-2}(-2) \;\; \cdots \;\; g^*_{l,0}(-N_g) \right]^T . \qquad (14)$$

Note the decreasing epoch index of the vector elements. Thus, the matched filter needs the N_g previous snap-shot channel estimates.

The SCAF vector is a $[(2\tilde{N}_g + 1) \times 1]$ column vector, where $\tilde{N}_g = N_g/2$ for even N_g. The solution requires $N_f - 1$ previous SCAF vectors which can be determined as,

$$\psi_i(r) = \sum_{l=1}^{L} \sum_{j=|i|}^{N_g-1-|i|} g^*_{l,j-i}(j - N_g - i(2r+1)) \cdot g_{l,j+i}(j - N_g - i(2r+1)) , \qquad (15)$$

for $i = -\tilde{N}_g, \ldots, 0, \ldots, \tilde{N}_g$, and for $r = 0, -1, \ldots, -N_f + 1$. Note that (15) requires all the channel variation during the decision delay $\Delta T/2$.

Then, the i-th row and j-th column element of correlation matrix R is

$$\sum_{q=-\tilde{N}_g}^{(N_f-1)-\max(i,j)} \psi_{q+i}(-j) \cdot \psi_{q+j}(-i) + \sigma_n^2 \psi_{j-i}(-j) , \qquad (16)$$

where $i, j = 0, 1, \ldots, N_f - 1$. The cross correlation column vector $\underline{P}$ is identified as

$$\psi_{N_f-1-i}(-i), \; i = 0, 1, \ldots, N_f - 1. \qquad (17)$$

Finally, for the $[N_b \times N_f]$ matrix B in the feedback part is, for $i = 0, 1, \ldots, N_b$, and $j = 0, 1, \ldots, N_f$,

$$\psi_{N_f+j-i}(-i) . \qquad (18)$$

Then, the feedforward and feedback filters can be determined from using (16)~(18), i.e., solving $R\underline{V}^* = \underline{P}$ and $\underline{w}_b^* = -B\underline{V}^*$. Note that the correlation matrix R is non-Toeplitz in general. Ignoring all the time epoch terms, i.e., using only one snap-shot channel vector, the correlation matrix becomes Toeplitz. We refer to this conventional solution as Toeplitz DFE (T-DFE) in this paper.

In summary, fast fades can be tracked using the NT-DFE. The NT-DFE is optimal since it uses all the channel state information during the decision delay and thus can be used as a benchmark to identify the sources of errors. The T-DFE uses only partial information and is thus suboptimal but has lower complexity than the optimal NT-DFE.

V. SYSTEM SIMULATION AND RESULTS

The performance of the diversity combining DFE system is investigated through complex base band computer simulations. A Monte Carlo approach with 2000-50,000 independent trials is used. To evaluate the adaptation, each trial consists of 5-16 frames, where a frame is a block of B symbols including the Nt training symbols. The main modulation scheme used is QPSK, but also included is the simulation of DQPSK for the purpose of easy comparison to the existing literature. In fact, the DQPSK result is about 2 dB worse than that of the QPSK, not 3 dB since the errors tend to occur in bursts in a long deep fade. The transmit filter with the square root raised cosine impulse response with a roll-off β (= 0.35) is realized with a *T/2-spaced* 31 tapped delay line filter (i.e., 15 symbols length truncation) with its energy normalized to 1. The SNR in this section implies the long term average SNR of the three path fading channel.

In Fig. 3 and Fig. 4, performances of three different channel estimation and tracking schemes are compared. ML or MAP refer to the MLE or MAP channel estimation and interpolation with NT-DFE with $(N_g, N_f, N_b) = (20, 5, 5)$. We refer to this method as tracking by interpolation (TI). RLS refers to the use of RLS channel tracking T-DFE without interpolation. Research reported in [3,10] indicate the channel-estimate based DFE is superior to the conventional direct adaptation of the DFE coefficients. Thus, exponential windowing RLS channel

tracking is considered here for a comparison with our proposed scheme. To be a fair comparison, the same known training blocks are inserted in the data stream. Thus, during the training mode the RLS algorithm and DFE filters are refreshed at the same rate. Furthermore, the exponential weighting factor (ω) of the RLS algorithm is optimized at various SNRs, fade rates, and channel lengths. For this, the following equation is adopted from [10],

$$SNR = \frac{(Nc+1)}{(2f_{dm}\pi T)^2}\frac{(1-\omega)^3}{(1+\omega)^2}. \quad (19)$$

The other simulation parameter is block length B = 80. RLS and TI curves show comparable performance in slow fading but large differences in fast fading.

In Fig. 3, the RLS tracking T-DFE performance of DQPSK signaling is evaluated with $(N_g, N_f, N_b) = (12,4,4)$. Relying on the detected symbols to update the channel state, RLS cannot provide the channel information during the decision delay. Thus, only T-DFE can be considered with RLS channel tracking. However, using T-DFE a longer decision delay (longer receiver filter orders) might become counterproductive in fast fades (see [4] for details). Thus, shorter filter orders $(N_g, N_f, N_b) = (12, 4, 4)$ are found to be the optimum trading-off for the worst case fading at *fdm* = 100 *Hz*. We see that at *fdm* = 100 *Hz* the irreducible BER is too high (0.1 for $L = 1$ and 0.01 for $L = 2$) to be of any practical use. Therefore, we confirm that RLS actually fails to track the fast Rayleigh fading channel.

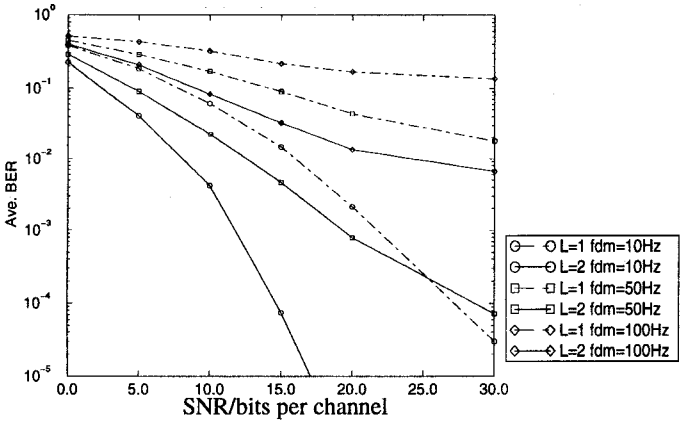

Fig. 3 Ave. DQPSK BER: RLS channel tracking T-DFE

In contrast, TI-NT-DFE curves in Fig. 4 show a superior and robust BER performance against fast fading. The TI-NT-DFE BER curves for *fdm* = 100 *Hz* are not even flat out up to 30 *dB*. Moreover, for the Ideal

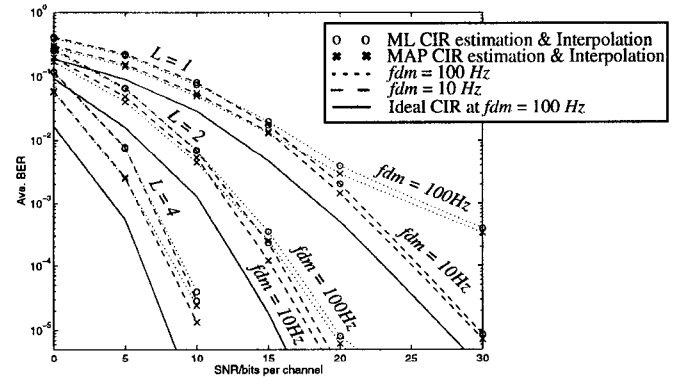

Fig. 4 Ave. DQPSK BER of training & interpolation channel tracking

CIR case (true channel values are used) the BER curves for *fdm* = 100 *Hz* are almost identical to the ones for 10 *Hz*. That is, no error floor is experienced by the virtue of our newly developed non-Toeplitz computation of the DFE filter coefficients. This is a significant departure from the other published results [4,11] in which a DFE receiver whose coefficients are either updated from RLS or from direct calculations using the T-DFE exhibits relatively high irreducible BER floors in fast fading, even in an ideal channel reference mode. In addition, note that the throughput rate at this BER performance is $(B - Nt)/B$ = (80-11)/80 = 0.8625.

In Fig. 5, we wish to distinguish the causes of the BER floor at the fastest fading rate. In particular, the NT-DFE and the T-DFE are compared and also three methods of obtaining channel impulse responses are contrasted. The optimal filter orders for the T-DFE are again $(N_g, N_f, N_b) = (12, 4, 4)$. The filter orders used for the NT-DFE are (20, 5, 5). The perfect CIR & interpolation in the figure implies tracking by interpolation on a set of perfect channel estimates, i.e., no errors in the periodic channel estimation. Comparison of these curves would identify the main cause of the irreducible error at the high SNRs.

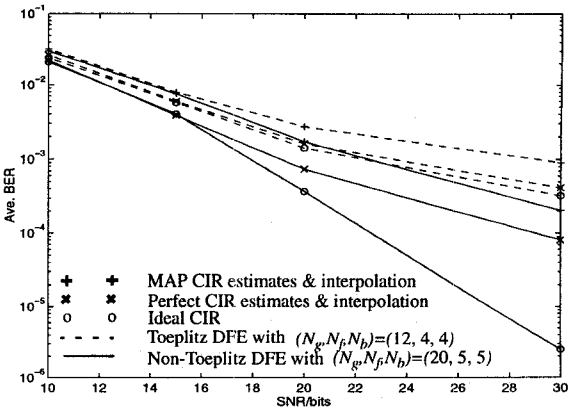

Fig. 5 Ave. QPSK BER simulation to determine the source of error floors

Not much difference is observed for low SNR. Thus, we pay attention to BERs at 30 *dB*. First, note that the T-DFE curves entail higher BER floors. Even the perfect CIR-T-DFE produces a higher BER floor than the MAP-NT-DFE does. This illustrates the detrimental consequence of ignoring the channel variation during the decision delay in the DFE coefficient computation. Second, comparing the non-Toeplitz curves it is demonstrated that the irreducible BER floors are mainly due to the interpolation errors. The interpolator performs poorly in the middle of the data segment, thus, the decision errors occur predominantly during the middle of the data frame. This problem persists even at B = 40 for which the BER at 30 *dB* is about 3×10^{-5} (not shown in the figures). This is improved but could still be made better

In Fig. 6, the sensitivity of increasing the DFE update periods μ is investigated at the fastest fading rate of *fdm*=100 *Hz*, where μ is the number of symbol periods between the DFE coefficients updates. Again, the BER performances of the two matched filtered DFE methods are compared, Toeplitz and non-Toeplitz. We use again the optimal filter orders, $(N_g, N_f, N_b) = (12, 4, 4)$ for the Toeplitz case. For the non-Toeplitz case, (20, 5, 5) are used for $\mu = 1$, while shorter filters of (16, 4, 4) for other values of μ. The MAP estimator is used for the both. First, the performance difference of the two deepens for a higher diversity order and for higher SNR, whereas it becomes almost negligible for $L = 1$ and for low SNR. Second, the non-Toeplitz methods maintain its superiority to the Toeplitz only for a small μ, i.e., for $\mu \geq 5$ the BER gain quickly disappears. Thus, if a large μ has to be chosen for a lower computational complexity, then the use of T-DFE is adequate.

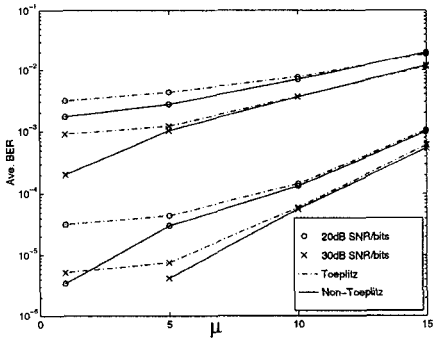

Fig. 6 Ave. QPSK BER vs. the DFE filter update period (μ) of training & interpolation schemes.

Finally, in Table 1 we tabulate example calculations of computational requirements for each algorithm, i.e., the number of multiplications/ divisions for RLS-T-DFE, TI-T-DFE, and TI-NT-DFE. Assuming a T/2-sampled sinc function is stored, the interpolated overall CIR estimates of $\hat{\underline{g}}$ can be obtained with $N_R(Q+N_g)$ complex multiplications, i.e., the interpolated channel vector $\hat{\underline{b}}$ can be obtained from $N_R Q$ complex multiplications and the convolution of $\underline{b}$ and $\underline{f}$ requires another $N_R N_h$. No computation is required to obtain the matched filter coefficient vector $M_f(k)$ since we can get it from the channel estimates without calculation. The computational burden to obtain the updated optimal filter vector $\underline{V}(k)$ might be high for a large N_f. Computationally efficient methods can be used such as the Cholesky factorization for the NT-DFE and the Levinson-Durbin algorithm for the T-DFE, which usually require on the order of N_f^3 and N_f^2 complex multiplications [7] to obtain $\underline{V}(k)$. If these numbers are still too large, further savings can be achieved by increasing the filter update period μ (e.g., μ = 5 symbols). In such a case, the obvious choice is the T-DFE since the performance gain of the NT-DFE quickly disappears with increase of μ as shown in Fig. 6. The example calculations are for $(N_g, N_f, N_b, N_c, Q, B, Nt) = (12, 4, 4, 6, 4, 80, 11)$.

TABLE 1. Number of multiplications/divisions

L	RLS channel tracking T-DFE	TI channel tracking T-DFE	TI channel tracking NT-DFE
1	279 (147)	263 (53)	464
2	465 (271)	436 (88)	714

VI. CONCLUDING REMARKS

We have presented robust channel estimation and tracking methods which require little system overhead over the fast Rayleigh fading dispersive channel. It has been explicitly shown through simulations that the tracking by interpolation method with our proposed channel estimation methods is significantly better than the RLS channel tracking method and than the previously published block CIR estimation methods, in terms of both the throughput and the BER performance. Our proposed reduced dimension CIR estimation allows us to employ shorter training sequences while maintaining the level of performance at a satisfactory level.

We have derived the NT-DFE which takes into account the channel variation during the decision delay. The training and interpolation scheme can provide the channel variation information during the decision delay. Thus the NT-DFE can obtain the full benefit of the channel interpolation. As the result, unlike previous published results, even for the fast fading at the normalized fading rate of 0.0042 the NT-DFE produces no BER floors in an ideal channel reference mode. The optimal the NT-DFE incurs relatively high computational complexity, and thus for a suboptimal but low complexity solution we propose the use of T-DFE which provides performance better than RLS type adaptations with less complexity.

For higher SNR, however, the curves still become flat. The reason for this error floor is identified as the interpolation errors, especially during the middle of the data frame. Design of interpolators to overcome this problem would be an interesting research exercise.

REFERENCES

[1] D.D. Falconer, Fumiyuki Adachi, and Bjorn cudmundson, "Time Division Multiple Access Methods for Wireless Personal Communications," *IEEE Comm. Mag.*, pp. 50-57, Jan. 1995.

[2] S.N. Crozier, Short-Block, Data Detection Techniques Employing Channel Estimation for Fading, Time-Dispersive Channels, PhD thesis, Dept. of Systems and Computer Engineering, Carleton University, Ottawa, ON, Canada, May 1990.

[3] G.W. Davidson, D.D. Falconer and A.U.H. Sheikh, "An investigation of block-adaptive decision feedback equalization for frequency selective fading channels," *Can.J.Elect. & Comp. Eng.*, Vol. 13, no. 3-4, 1988.

[4] S. Fechtel and Heinrich Meyr, "An investigation of channel estimation and equalization techniques for moderately rapid fading HF-channels," in *Proc. ICC* '91, pp. 768-772.

[5] N.W.K. Lo, D.D. Falconer and A.U.H. Sheikh, "Adaptive Equalization and Diversity Combining for Mobile Radio using Interpolated Channel Estimates," *IEEE Trans. Vehic. Tech.*, vol. VT-40, no.3, pp. 636-645, Aug. 1991.

[6] R. Steel, Mobile Radio Communications. New York: IEEE press, 1992.

[7] J.G. Proakis, *Digital Communications.* New York, NY: McGraw-Hill, 1983.

[8] W.C. Jakes, ed., *Microwave Mobile Communications.* New York, NY: Wiley, 1974.

[9] H. Lee and G. Pottie, "Fast adaptive equalization/diversity combining for time-varying dispersive channels," submitted to *IEEE Trans. Comm.*, 1996.

[10] P.K. Shukla and L.F. Turner, "Channel-estimation-based adaptive DFE for fading multipath radio channels," *IEE Proceedings-I,* vol. 138, no.6, pp., 525-543, Dec. 1991.

[11] E. Eleftheriou and D.D. Falconer, "Adaptive Equalization Tech. for HF channels", *IEEE J. Sel. Areas in Comm.*, vol. SAC-5, no.2, pp.238-247, Feb. 1987.